



Lateral-Torsional Buckling of Simply Supported Anisotropic Steel-FRP Beams under Pure Bending Condition

Hayder A. Rasheed¹, Habiburrahman Ahmadi², AlaaEldin Abouelleil²

Abstract

In this paper, a generalized analytical approach for lateral-torsional buckling of simply supported anisotropic hybrid (steel-FRP), thin-walled, rectangular cross-section beams under pure bending condition was developed using the classical laminated plate theory as a basis for the constitutive equations. Buckling of such type of hybrid members has not been addressed in the literature. The hybrid beam, in this study, consists of a number of layers of anisotropic fiber reinforced polymer (FRP) and a layer of isotropic steel sheet. The isotropic steel sheet is used in two configurations, (i) in the mid-depth of the beam sandwiched between the different FRP layers and (ii) on the side face of the beam. A closed form buckling expression is derived in terms of the lateral, torsional and coupling stiffness coefficients of the overall composite. These coefficients are obtained through dimensional reduction by static condensation of the 6x6 constitutive matrix mapped into a 2x2 coupled weak axis bending-twisting relationship. The stability of the beam under different geometric and material parameters, like length/height ratio and ply orientation, was investigated. The analytical formula is verified against finite element buckling solutions using ABAQUS for different lamination orientations showing excellent accuracy.

Keywords: lateral-torsional buckling, stability, thin-walled beam, anisotropic laminated composite, hybrid laminated beam, finite element method.

2. Introduction

A thin-walled slender beam subjected to bending moments about the strong axis may buckle by a combined lateral bending and twisting of the cross-section. This phenomenon is known as lateral-torsional buckling. Theory of thin-walled open section beams including axial constraints for isotropic materials was developed by Vlassov (1961). This classical theory neglects the shear deformation in the middle surface of the wall so that for the composite beams, the shear deformations may significantly increase the displacements and reduce the buckling loads. The shear deformation theory for transversely loaded isotropic beams was developed by Timoshenko and Gere (1961).

¹ Professor, Kansas State University, <Email: hayder@ksu.edu, Tel: 785-532-1589>

² Graduate Research Assistant, Kansas State University

Many researchers then started to study the lateral torsional buckling for the laminated composite beams using different theoretical approaches and enhancing their work with experimental programs and finite element models to validate the theory. Lin et al. (1996) studied the stability of thin-walled composite member using the finite element method. Seven degrees of freedom at each node for each two noded elements were used to model the fiber reinforced plastic. The seven degrees of freedom are the dependent translations in three perpendicular directions and the corresponding rotations in addition to the angle of warping. The stiffness matrices of a beam element were used to develop the element shape functions. A number of examples of thin walled-open sections were solved, different cross sections like channels, I sections, and Z-section were tested as well as different boundary conditions. The study concluded the importance of the influence of in-plane shear strain on the critical buckling load for lateral torsional buckling and combined torsional and flexural modes. It also minimized the significance of shear strain effect on critical buckling when the buckling happens in terms of a flexural mode. Davalos and Qiao (1997) used the non-linear elastic theory to develop a stability solution for lateral-distortional buckling for composite wide flange beams based on the principle of total potential energy. A fifth-order polynomial shape function was adopted for the displacement field construction. Then, the proposed model was validated against two geometrically identical experimental beams loaded at mid-span, with different material characteristics. A good agreement was obtained against the experimental results and a finite element model. Kollar (2000) presented a stability analysis of thin walled composite columns under axial loading conditions. A closed form solution was derived using a modified version of Vlasov's classical theory (1961) for isotropic material to account for the composite action. The effect of shear deformation in in-plane displacements and in the restrained warping was examined and a shear matrix was formulated in addition to the bending matrix. Lee et al. (2002) studied the lateral buckling of composite laminated beams. An analytical approach based on the classical lamination theory was derived for different boundary conditions and different laminate stacking sequences. The examined beams were tested under various loading configurations and various locations. The beams were then compared against a one dimensional finite element model under different load configurations. The model showed a good agreement against the finite element model of simply supported I beam in cases of pure bending, uniformly distributed loads, and central point load. Yet, the model was not appropriate for pure bending with off-axis fiber orientation due to coupling stiffness. Sapkas and Kollar (2002) offered closed form solutions for simply supported and cantilever, thin walled, open section, orthotropic composite beams subjected to concentrated end moments, concentrated forces, or uniformly distributed load. The solution indirectly accounted for shear deformation by adjusting the bending and warping stiffness of the composite beams. Qiao and Davalos (2003) formulated an analytical solution for flexural-torsional buckling of composite cantilever I beams based on an energy method developed from the non-linear plate theory. A good agreement against finite element method was obtained. Furthermore, four different cantilever beams were tested experimentally under tip loads to examine the flexural-torsional response. Also, good agreements were shown against the experimental results. Kotelko (2004) presented a theoretical analysis of local buckling which represents material failure. This study covered different cross sections of thin walled beams and columns. These cross sections varied between lipped and plain channels as well as box-section. This theory matched previous theories in a way that it depends on the rigid-plastic model. Yet, it mainly differs by considering a constitutive strain-hardening of the used material. This analytical approach is particularly useful in the initial phase of design process and may be applied as a simplified design tool at the

early stage of design process, including crush-oriented design. Karaagac et al. (2007) tested the stability of a cantilever laminated composite beam under static and dynamic conditions. A linear translation spring was attached to the beam to control the lateral deformation. The attached elastic support location varied between the free end and the mid-span of the beam. Length-to-thickness ratio, variation of cross-section in one direction, orientation angle, static and dynamic load parameters, stiffness and position of the elastic support were the main variables to study the stability of the beam. Numerical polynomial approximations for the displacements and the angle of twist were derived and showed a reasonable accuracy against the finite element method. Machado (2010) derived an analytical solution for lateral stability of cross-ply laminated thin-walled simply supported bisymmetric beams subjected to combined axial and bending loads. The presented theory included shear deformability and took into account large displacements and rotations; moderate bending rotations and large twisting angles. The proposed solution also examined the nonlinear pre-buckling geometrical deformation for more accurate representation of the lateral stability conditions. The buckling loads obtained analytically were, in general, in good agreement with the bifurcation loads observed in the post buckling response. The study concluded that the buckling moments computed from classical theory is overestimated. Also, it presented pre-buckling and post buckling displacement curves to relate the stiffness behavior of the beam to the applied loads and also to study the fiber orientation against the buckling loads.

In this study, an analytical model applicable to the lateral-torsional buckling of simply supported anisotropic hybrid (steel-FRP), thin-walled, rectangular cross-section beams, subjected to pure bending is developed. This model is based on the classical plate lamination theory (CPT), and accounts for the arbitrary laminate stacking sequence configurations. The analyzed beams consist of six layers of fiber reinforced polymer (FRP) sheets and one isotropic steel sheet. The FRP sheets have the same thickness and the same characteristics, yet they vary in terms of fiber angle orientation. The location of the steel sheet was examined in order to understand its influence on the lateral torsional buckling critical moment. A sandwich stacking configuration (ST-I) is defined by placing the steel sheet in the mid-thickness of the beam. A sided stacking configuration (ST-II) is defined by placing the steel sheet at the side face of the beam. A series of FRP angle configurations were determined for comparisons against a finite element model and also to compare the different configurations against each other. The finite element model is developed in ABAQUS to predict critical buckling moments and compare with the results obtained from the analytical model. Also, the length of the beam to its height ratio was examined to study the effect of beam size on the lateral torsional buckling resistance.

2. Analytical Formulation

A simply supported hybrid (steel-FRP) laminated composite beam with length L and a thin rectangular cross section is subjected to pure bending at the ends, as shown in Figure 1. The beam tends to buckle under a lateral-torsional behavior because of its small thickness.

The model in this study is based on the classical plate lamination theory, Kollar (1999) and Barbero (1999), which is derived from plane stress state, and all the assumptions in classical plate theory remain valid for laminated composite thin-walled beams.

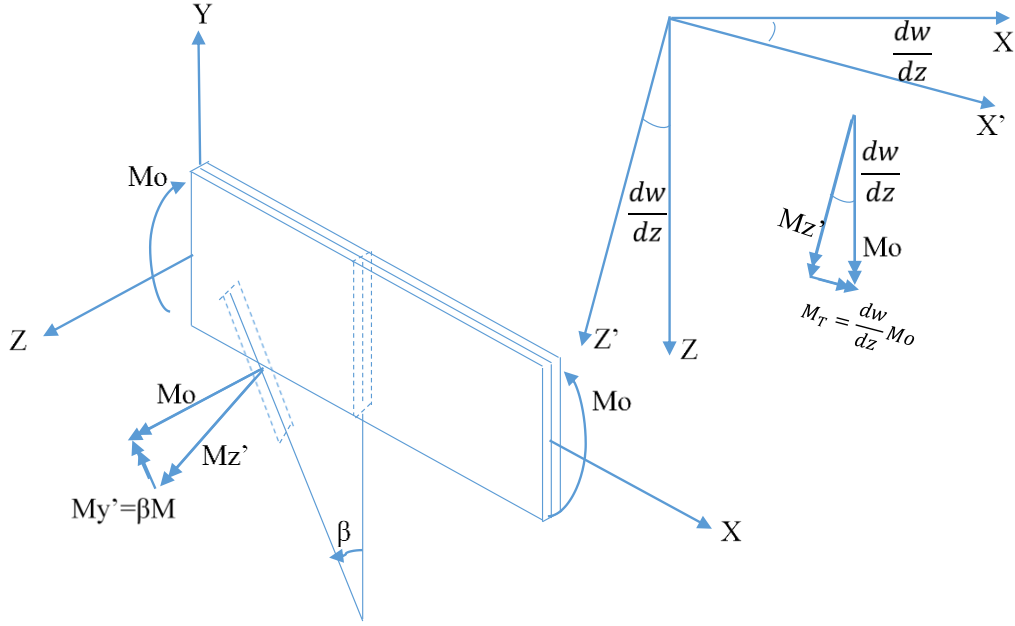


Figure 1: A deformed laminated beam subjected to pure bending (structural coordinate system)

3.1 Kinematics

Based on the assumptions in the classical plate theory, the displacement components u , v , w representing the deformation of a point on the plate profile section are given with respect to mid-surface displacements u_0 , v_0 , and w_0 as follows:

$$u(x, y, z) = u_0(x, y) - z \frac{dw_0}{dx}(x, y) \quad (1)$$

$$v(x, y, z) = v_0(x, y) - z\beta(x, y) \quad (2)$$

$$w(x, y, z) = w_0(x, y) \quad (3)$$

Where $\beta = \frac{\partial w_0}{\partial y}$

The strains associated with small displacements from the theory of elasticity are given by

$$\varepsilon_x = \varepsilon_x^0 + z\kappa_x \quad (4)$$

$$\varepsilon_y = \varepsilon_y^0 + z\kappa_y \quad (5)$$

$$\gamma_{xy} = \gamma_{xy}^0 + z\kappa_{xy} \quad (6)$$

where

$$\varepsilon_x^0 = \frac{\partial u_0}{\partial x}, \varepsilon_y^0 = \frac{\partial v_0}{\partial y} \quad (7)$$

$$\kappa_x = -\frac{\partial^2 w_0}{\partial x^2}, \kappa_y = -\frac{\partial \beta}{\partial y}, \text{ and } \kappa_{xy} = -2\frac{\partial \beta}{\partial x} \quad (8)$$

3.2 Stress-Strain Equations

The stress-strain relation for a layer is derived in the state of plane stress. For an isotropic material, the stress-strain relation is as follow:

$$\begin{Bmatrix} \sigma_x \\ \sigma_y \\ \tau_{xy} \end{Bmatrix} = \begin{bmatrix} \bar{E} & \bar{E}\nu & 0 \\ \bar{E}\nu & \bar{E} & 0 \\ 0 & 0 & G \end{bmatrix} \begin{Bmatrix} \epsilon_x \\ \epsilon_y \\ \gamma_{xy} \end{Bmatrix} \quad (9)$$

where $\bar{E} = \frac{E}{1-\nu^2}$ and $G = \frac{E}{2(1+\nu)}$

For anisotropic material, the stress-strain relation in the beam coordinate system is defined as follows:

$$\begin{Bmatrix} \sigma_x \\ \sigma_y \\ \tau_{xy} \end{Bmatrix} = \begin{bmatrix} \bar{Q}_{11} & \bar{Q}_{12} & \bar{Q}_{16} \\ \bar{Q}_{12} & \bar{Q}_{22} & \bar{Q}_{26} \\ \bar{Q}_{16} & \bar{Q}_{26} & \bar{Q}_{66} \end{bmatrix} \begin{Bmatrix} \epsilon_x \\ \epsilon_y \\ \gamma_{xy} \end{Bmatrix} \quad (10)$$

Where $[\bar{Q}_{ij}]$ are the components of the transformed reduced constitutive matrix which are given in standard textbooks like Kollar (1999) and Barbero (1999).

3.3 Force-Strain Equations

The plate stiffness coupling equations based on Classical Lamination Theory, shown in Figure 2, are given as follows.

$$\begin{Bmatrix} N_x = 0 \\ N_y = 0 \\ N_{xy} = 0 \\ M_x \neq 0 \\ M_y = 0 \\ M_{xy} \neq 0 \end{Bmatrix} = h \begin{bmatrix} A_{11} & A_{12} & A_{16} & B_{11} & B_{12} & B_{16} \\ A_{12} & A_{22} & A_{26} & B_{12} & B_{22} & B_{26} \\ A_{16} & A_{26} & A_{66} & B_{16} & B_{26} & B_{66} \\ B_{11} & B_{12} & B_{16} & D_{11} & D_{12} & D_{16} \\ B_{12} & B_{22} & B_{26} & D_{12} & D_{22} & D_{26} \\ B_{16} & B_{26} & B_{66} & D_{16} & D_{26} & D_{66} \end{bmatrix} \begin{Bmatrix} \epsilon_x \\ \epsilon_y \\ \gamma_{xy} \\ \kappa_x \\ \kappa_y \\ \kappa_{xy} \end{Bmatrix} \quad (11)$$

Where

$$A_{ij} = \sum_{k=1}^N (\bar{Q}_{ij})_k t_k \quad i, j = 1, 2, 6 \text{ are called extensional stiffness coefficients}$$

$$B_{ij} = \sum_{k=1}^N (\bar{Q}_{ij})_k t_k \bar{z}_k \quad i, j = 1, 2, 6 \text{ are called extension-bending coupling stiffness coefficients and}$$

$$D_{ij} = \sum_{k=1}^N (\bar{Q}_{ij})_k \left(t_k \bar{z}_k^2 + \frac{t_k^3}{12} \right) \quad i, j = 1, 2, 6 \text{ are called bending stiffness coefficients}$$

$(\bar{Q}_{ij})_k$ are the components of the k^{th} layer transformed reduced stiffness matrix in the beam coordinate system.

\bar{z}_k is the depth from the middle surface to the centroid of the k^{th} layer, and t_k is the thickness of k^{th} layer of the hybrid beam.

Knowing the zero components of externally applied forces and moments for the pure bending condition from Figure 1, which are expressed in Eq. 11, the stiffness matrix can be simplified and dimensionally reduced to an effective 2x2 stiffness matrix by using the static condensation technique:

$$\begin{Bmatrix} M_x \\ M_{xy} \end{Bmatrix} = h \begin{bmatrix} D_Y & D_{YT} \\ D_{YT} & D_T \end{bmatrix} \begin{Bmatrix} \kappa_x \\ \kappa_{xy} \end{Bmatrix} \quad (12)$$

where

$$\begin{bmatrix} D_Y & D_{YT} \\ D_{YT} & D_T \end{bmatrix} = \begin{bmatrix} D_{11} & D_{16} \\ D_{16} & D_{66} \end{bmatrix} - \begin{bmatrix} B_{11} & B_{16} \\ B_{12} & B_{26} \\ B_{16} & B_{66} \\ D_{12} & D_{26} \end{bmatrix}^T \begin{bmatrix} A_{11} & A_{12} & A_{16} & B_{12} \\ A_{12} & A_{22} & A_{26} & B_{22} \\ A_{16} & A_{26} & A_{66} & B_{26} \\ B_{12} & B_{22} & B_{26} & D_{22} \end{bmatrix}^{-1} \begin{bmatrix} B_{11} & B_{16} \\ B_{12} & B_{26} \\ B_{16} & B_{66} \\ D_{12} & D_{26} \end{bmatrix}$$

D_Y is the effective hybrid (steel-FRP) composite lateral stiffness coefficient, D_T is the effective hybrid composite twisting stiffness coefficient, and D_{YT} is the effective hybrid composite lateral-twisting coupling coefficient. In most cases, where the layers are symmetric, anti-symmetric, cross-ply, special angle ply, D_{YT} coefficient will be zero. However, for the generally anisotropic cases, D_{YT} coefficient is not zero and will play a significant role in determining the buckling moments of the beams.

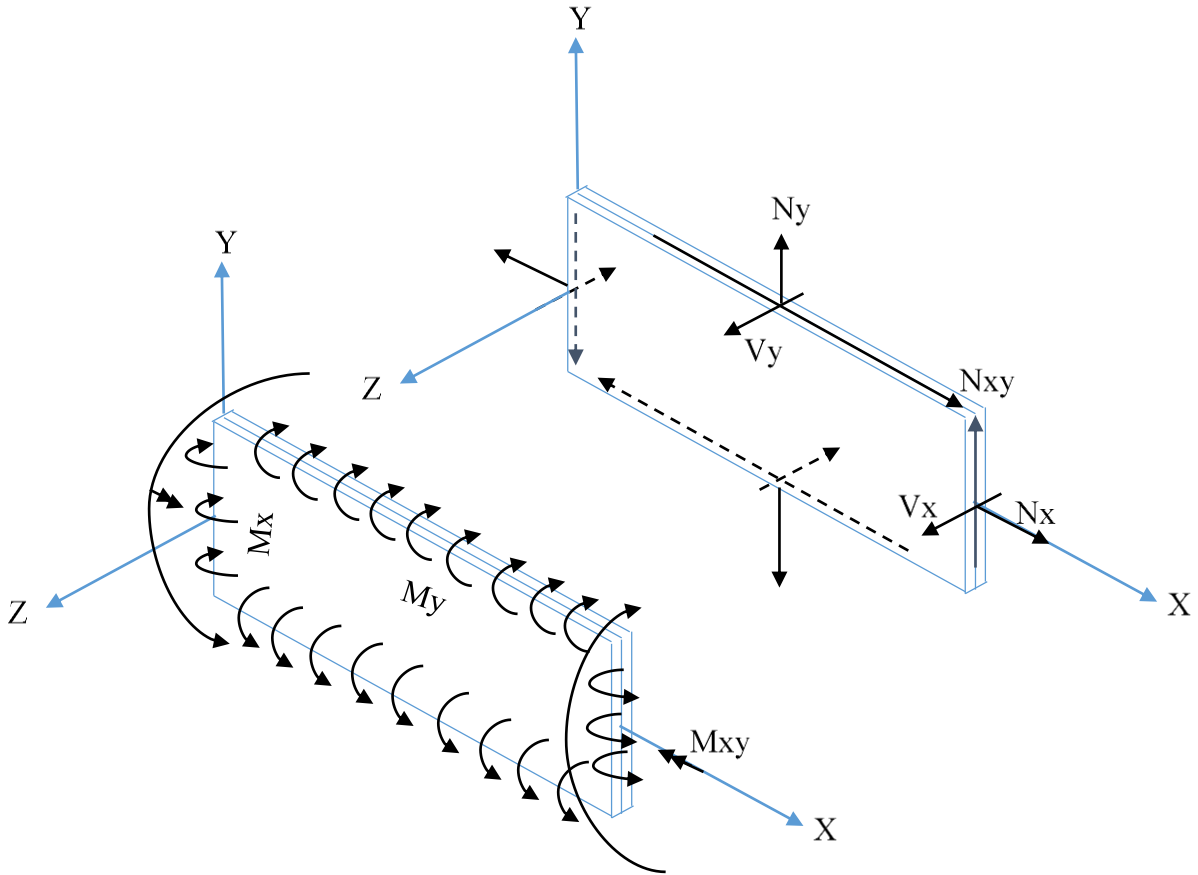
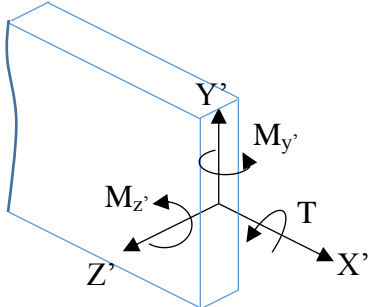
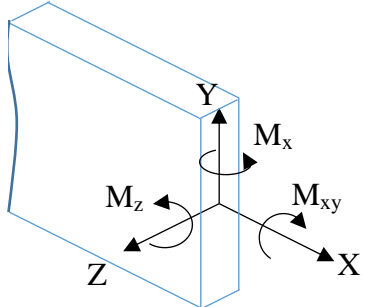


Figure 2: Force and moment resultants on a beam based on classical plate theory (laminated coordinate system).

Referring to Figure 1 (structural coordinate) and Figure 2 (laminated coordinate), the bending moment M_y in structural coordinate is replaced by M_x in laminate coordinate. On the other hand, the shear moment, M_{xy} , in laminate coordinate is in the opposite direction of twisting moment in the structural coordinate system and is found by Kollar (1999) to be $T = -2 M_{xy}$. Table 1 shows the relation of moment components in structural coordinate and laminate composite coordinate.

Table 1 relation of moment components in structural coordinate and laminate composite coordinate	
The structural coordinate (deformed axes)	Laminate composite coordinate
	<div style="text-align: center;"> $\begin{aligned} M_z' &= M_z \\ M_y' &= M_x \\ T &= -2M_{xy} \end{aligned}$ </div> 

Substituting the curvatures in terms of displacement and rotation in Eq. 8 into Eq. 12, and writing the moments in structural coordinates systems, the following relation will be obtained

$$\begin{Bmatrix} M_{y'} \\ -M_T \end{Bmatrix} = h \begin{bmatrix} D_Y & 2D_{YT} \\ 2D_{YT} & 4D_T \end{bmatrix} \begin{Bmatrix} -\frac{d^2w}{dx^2} \\ -\beta' \end{Bmatrix} \quad (13)$$

3.4 Equilibrium Equations:

Figure 1 shows the components of external moments before and after deformation and is obtained as follows:

External moments in un-deformed configuration (original axes):

$$M_z = M_o \text{ (Applied Moment)} \quad (14a)$$

$$M_T = M_y = 0 \quad (14b)$$

External moments in the deformed configuration (deformed axes):

$$M_z' = M_z = M_o \quad (15a)$$

$$M_y' = \beta M_o \quad (15b)$$

$$M_T = M_x' = \frac{dw}{dx} M_o \quad (15c)$$

The following system of differential equation is obtained after substituting the external moments from Eq. 15b and c into Eq. 13:

$$\begin{Bmatrix} \beta M_o \\ -\frac{dw}{dx} M_o \end{Bmatrix} = h \begin{bmatrix} D_Y & 2D_{YT} \\ 2D_{YT} & 4D_T \end{bmatrix} \begin{Bmatrix} -\frac{d^2w}{dx^2} \\ -\beta' \end{Bmatrix} \quad (16)$$

$$-hD_Y \frac{d^2w}{dx^2} - 2hD_{YT}\beta' = \beta M_o \quad (17)$$

$$-2hD_{YT} \frac{d^2w}{dx^2} - 4hD_T\beta' = -\frac{dw}{dx} M_o \quad (18)$$

Writing Eq.17 and Eq.18 in terms of $\frac{d^2w}{dx^2}$ and equating the two expressions, the following relationship can be obtained.

$$\frac{1}{hD_Y} [-2hD_{YT}\beta' - \beta M_o] = \frac{1}{2hD_{YT}} \left[-4hD_T\beta' + \frac{dw}{dx} M_o \right] \quad (19)$$

Differentiating Eq.19 with respect to x and rearranging the resulting expression in terms of $\frac{d^2w}{dx^2}$, Eq.20 will be obtained.

$$\frac{d^2w}{dx^2} = -\frac{2D_{YT}}{D_Y} \beta' + \frac{4h}{M_o} \left[D_T - \frac{D_{YT}^2}{D_Y} \right] \beta'' \quad (20)$$

Equating the left hand side of Eq.19, which is equal to $\frac{d^2w}{dx^2}$ in Eq. 17, and the right hand side of Eq.20, the resulting expression reduces to a second order ordinary differential equation with constant coefficients, which can be solved analytically.

$$\beta'' + \frac{M_o^2}{4h^2[D_Y D_T - D_{YT}^2]} \beta = 0 \quad (21)$$

setting $\kappa^2 = \frac{M_o^2}{4h^2[D_Y D_T - D_{YT}^2]}$, yields an equation similar to the isotropic condition when the warping effect is neglected.

$$\beta'' + \kappa^2 \beta = 0 \quad (22)$$

The general solution for this type of differential equation is known to be:

$$\beta = A \sin(kx) + B \cos(kx) \quad (23)$$

Applying boundary condition for pure bending as $\beta(0) = \beta(L) = 0$, the critical buckling moment is obtained according to the following equation.

$$M_{0cr} = \frac{\pi h}{L} \sqrt{4(D_Y D_T - D_{YT}^2)} \quad (24)$$

The critical moment for isotropic beam was obtained by Timoshenko and Gere (1961) as follows:

$$M_{0cr} = \frac{\pi}{L} \sqrt{EI_y GJ} \quad (25)$$

where $J = \frac{1}{3} h t^3$

For an isotropic material where $D_{YT} = 0$, the following relation is obtained.

$$EI_y = 2hD_Y \quad (\text{Lateral stiffness coefficient}) \quad (26)$$

$$GJ = 2hD_T \quad (\text{Torsional stiffness coefficient}) \quad (27)$$

3. Numerical Analysis (FEA)

The finite element method in the commercial software, ABAQUS/Standard (implicit) was used to simulate the problem in this study. The model was first created by using 3D planar shells. The shells were assembled based on the stacking arrangement that was used in the analytical solution.

The global x-axis was used along beams length, but the local coordinate system was used based on the orientation of the fibers in each ply.

The boundary conditions for this beam were applied as follows. The four corners of the beam, shown in Figure 3, were constrained from moving in z-direction. One end of the beam was pinned at mid-height restraining it from all displacements, and a roller was applied at mid-height of other end of the beam to restrain displacement in the y-direction only, as shown in the Figure 3.

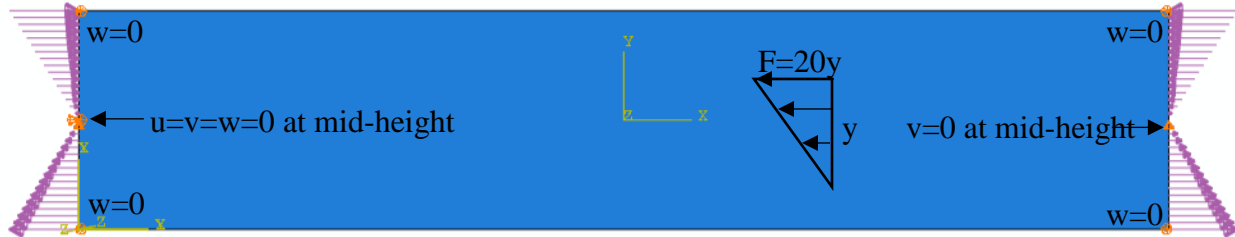


Figure 3 applied load and boundary conditions

A linear shell-edge load was applied at both ends of the beam as tension and compression stresses to create a pure bending moment condition in the beam, as shown in Figure 3. Each edge was partitioned into two parts to apply shell-edge load linearly in the desired direction. The following relation was used to determine the magnitude of the linear load.

$$F_x = 20y \quad (28)$$

There is no load applied at the mid-height of the edge and the load increases linearly by 20y, which will act as a pure bending moment when applied as compression above the mid-height and as tension below the mid-height.

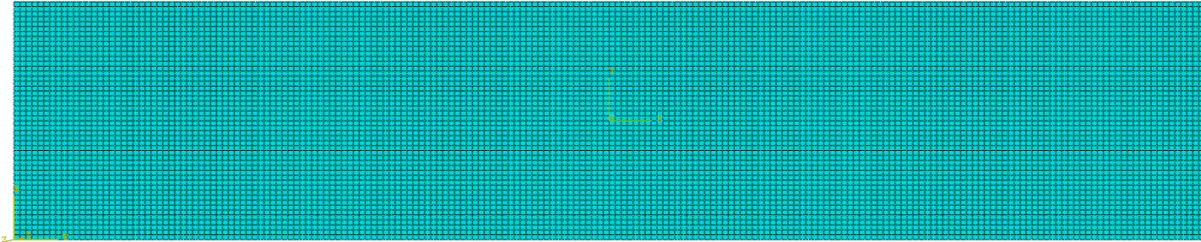


Figure 4: Applied shell element type (S8R) and mesh (element size along beam axis: 2.5 mm)

The beam was meshed with a standard quadratic quadrilateral shell element type of S8R (8-node doubly curved thick shell element with reduced integration) using six degrees of freedom per node and an element size of 2.5 mm along beam axis. A beam with $L = 500$ mm and $h = 100$ mm gives a total number of 29297 nodes and 9600 elements, as shown in Figure 4.

The eigenvalue buckling analysis in Abaqus solver, which is a linear perturbation procedure, determines the eigenvalue of the buckling mode. Abaqus extracts the eigenvalues and eigenvectors for symmetric stiffness matrices only. In order to make the stiffness matrix of the model symmetric, Lanczos iteration eigenvalue extraction method was used. To find the critical moment, based on the Abaqus user guide, the lowest eigenvalue is multiplied by the moment

which was applied at the ends of the beam in combined tension and compression line edge loading.

$$M_{ocr} = \lambda M_0 \quad (29)$$

Where M_0 is calculated from applied linear edge load.

4. Results

4.1 Material properties and stacking sequences

An anisotropic hybrid (steel-FRP) composite beam is made by stacking six layers of the FRP of lamina properties shown in Table 2 at different fiber orientations and one layer of isotropic steel sheet given in Table 3. The thickness of each layer along with steel sheet is the same, yet it varies in terms of fiber orientation. The orientation of fiber in each layer can be randomly picked, including common laminate types such as symmetric laminates, antisymmetric laminates, balanced laminates, and so on. Two stacking configurations were considered in order to place the steel sheet: (i) sandwich stacking (ST-I) where the steel sheet is placed at mid-depth of the beam and (ii) sided stacking (ST-II) where the steel sheet is placed in the front face of the beam. The stacking sequence starts from the back of the beam to the front of the beam to follow the same order used for typical laminated plates, Figure 5. For example, [30/-30/90/ST/30/-30/90] means that the first ply has an angle of 30 degrees from the x-axis of the beam is placed in the back of the beam counter clockwise (towards the y-axis) and the other layers follow with the same order through the positive z-axis, and ST indicates the location of isotropic steel sheet in the mid-depth. Figure 5 shows the stacking sequence of the laminates and location of steel sheet. Different length to height ratios of (5, 10, 20, and 50) were also studied which will be presented later.

Table 2: Material 1 (FRP) properties used the in laminates

Material	FRP	
E_{11}	142730	MPa
E_{22}	13790	MPa
ν_{12}	0.3	
ν_{21}	0.028985	
G_{12}	4640	MPa
G_{13}	4640	MPa
G_{23}	3030	MPa

Table 3: Material 2 (Steel) properties used the in laminates

Material	FRP	
E_{11}	200000	MPa
E_{22}	200000	MPa
ν_{12}	0.3	
ν_{21}	0.3	
G_{12}	76923.08	MPa
G_{13}	76923.08	MPa
G_{23}	76923.08	MPa

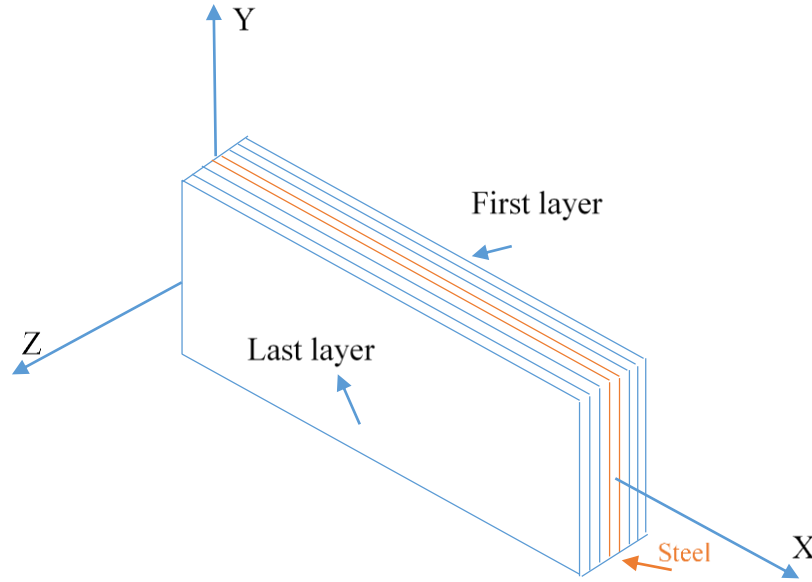


Figure 5: The stacking sequence of the laminate and location of steel sheet (ST-I)

4.2 Buckling Results

For the lateral-torsional buckling of thin-walled rectangular laminated composite beams under pure bending conditions, an analytical approach is presented as well as FEA results. Figure 6-9 show the buckling results for different stacking sequences based on the proposed analytical formulation and also results from FEA model. Fig. 6 and 7 show the results of ST-I (sandwich) configuration and ST-II (sided) configuration of 18 different laminate-fiber orientation for beam length to height ratio of 5. Similarly, Fig. 8 and 9 show the results of ST-I configuration and ST-II configuration of 18 different laminate-fiber orientation for beam length to height ratio of 20. The same comparison was held for beam length to height ratios of 10 and 50. Based on the results obtained, there is an excellent agreement between the proposed analytical formulation and FEA for all the orientations with an error that does not exceed 3.5% except for the zero fiber orientation. The largest error observed is 8.7% (Figure 6) for the 0/0/0/ST/0/0/0 case, which buckled in a distortional mode rather than lateral-torsional mode, which will be explained in details later in this paper, Fig. 18.

5. Parametric Study

5.1 Effect of Length/height ratio

Different Length/height (L/h) ratios of 5, 10, 20, and 50 were used in the analysis to study their effects on the lateral-torsional buckling of simply supported laminated thin-walled rectangular cross-sectional hybrid beams. The results show that there is a significant drop in the value of the buckling moments as the L/h ratio increases. The relation between buckling moment and L/h ratio is defined to be a power function which can be written in Eq. 30.

$$M_{cr} = (M_{cr})_i * \left(\frac{L}{h}\right)_i \left(\frac{L}{h}\right)^{-1} \quad (30)$$

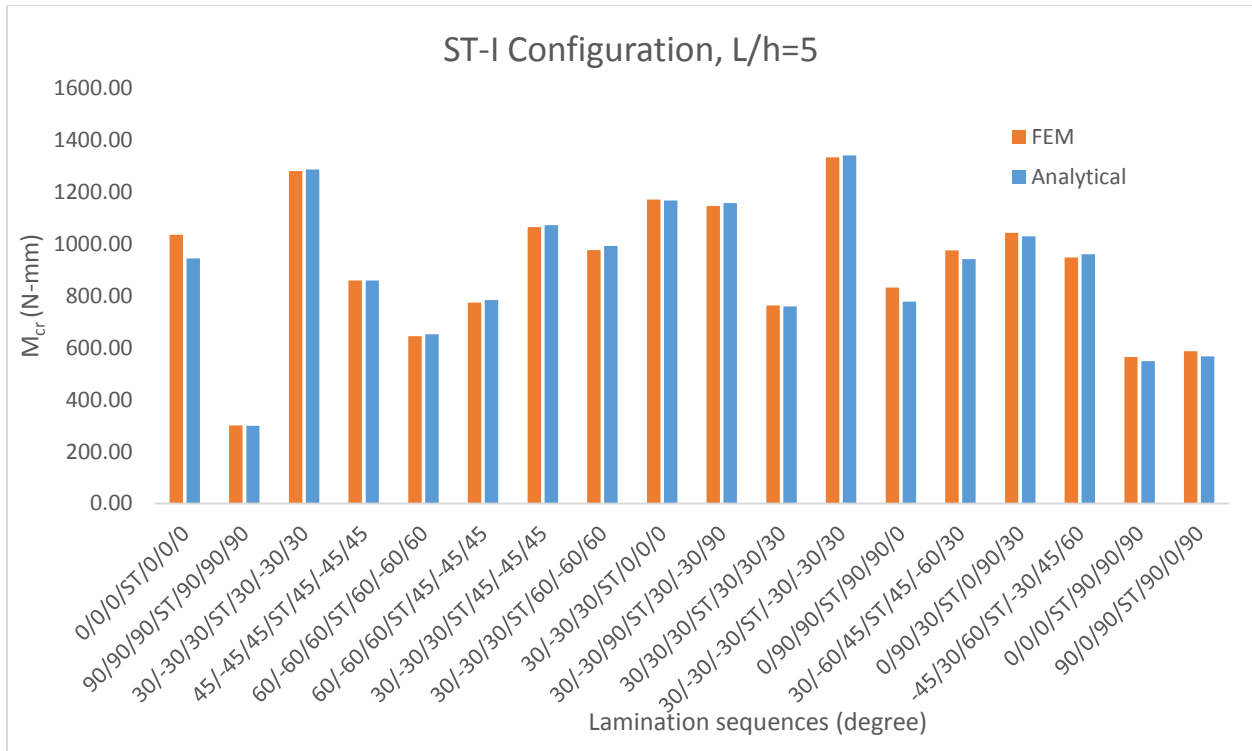


Figure 6: Buckling moments at different stacking sequences: $t_k=0.1$ mm for each layer, $L/h=5$, and ST-I configuration

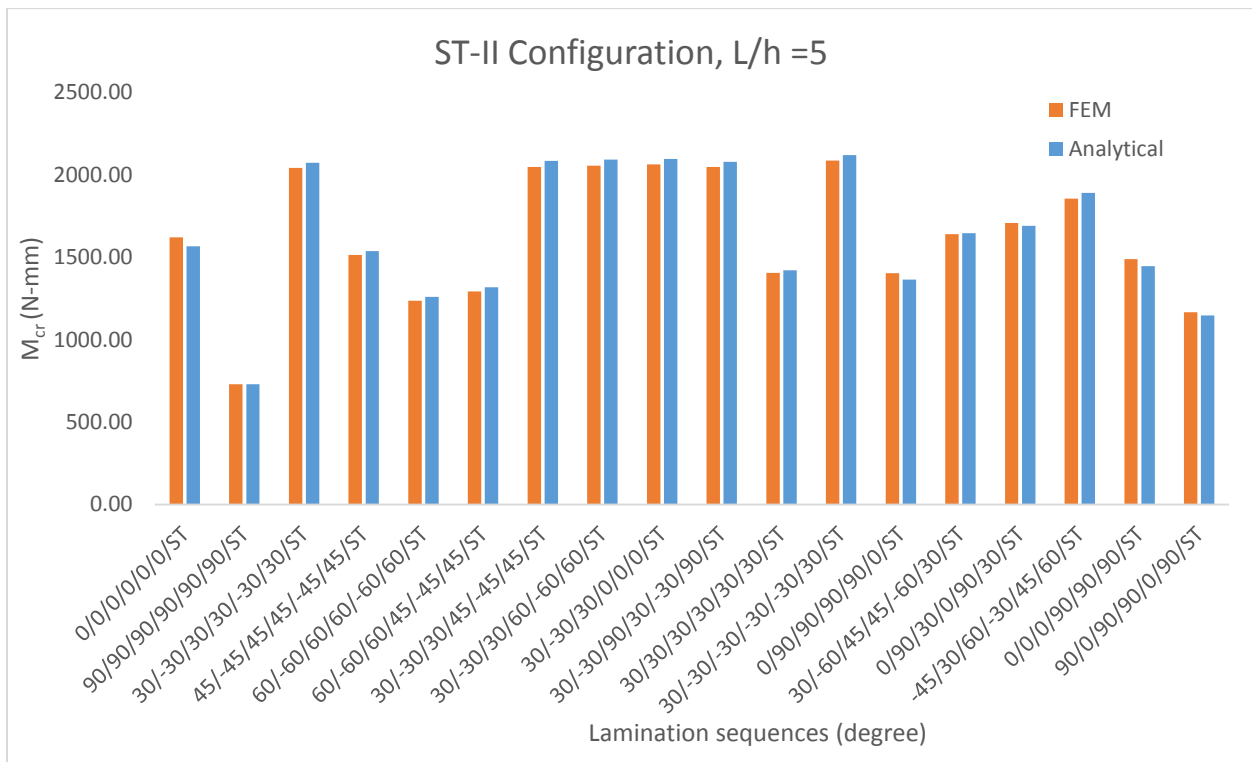


Figure 7: Buckling moments at different stacking sequences: $t_k=0.1$ mm for each layer, $L/h=5$, and ST-II configuration

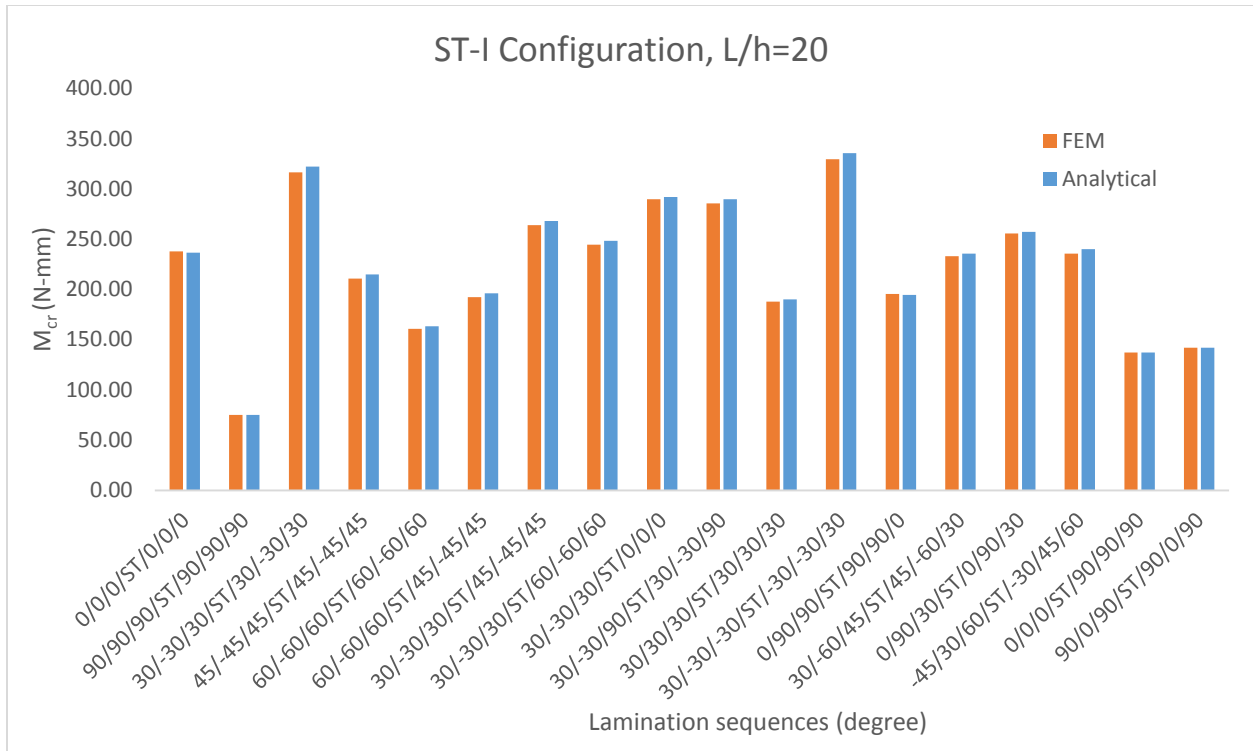


Figure 8: Buckling moments at different stacking sequences: $t_k=0.1$ mm for each layer, L/h=20, and ST-I configuration

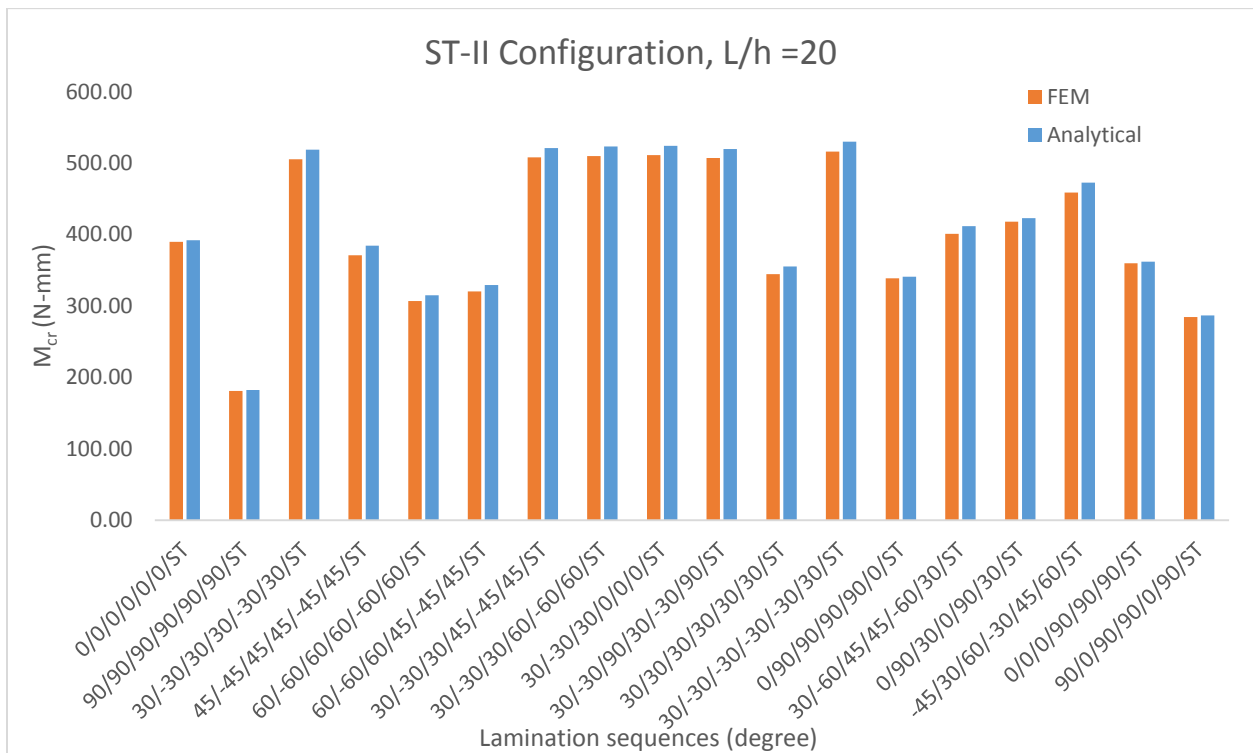


Figure 9: Buckling moments at different stacking sequences: $t_k=0.1$ mm for each layer, L/h=20, and ST-II configuration

Where $(M_{cr})_i$ is the initial calculated value of buckling moment from Eq. 30 with a given $(\frac{L}{h})_i$ ratio for a specific laminate stacking sequence.

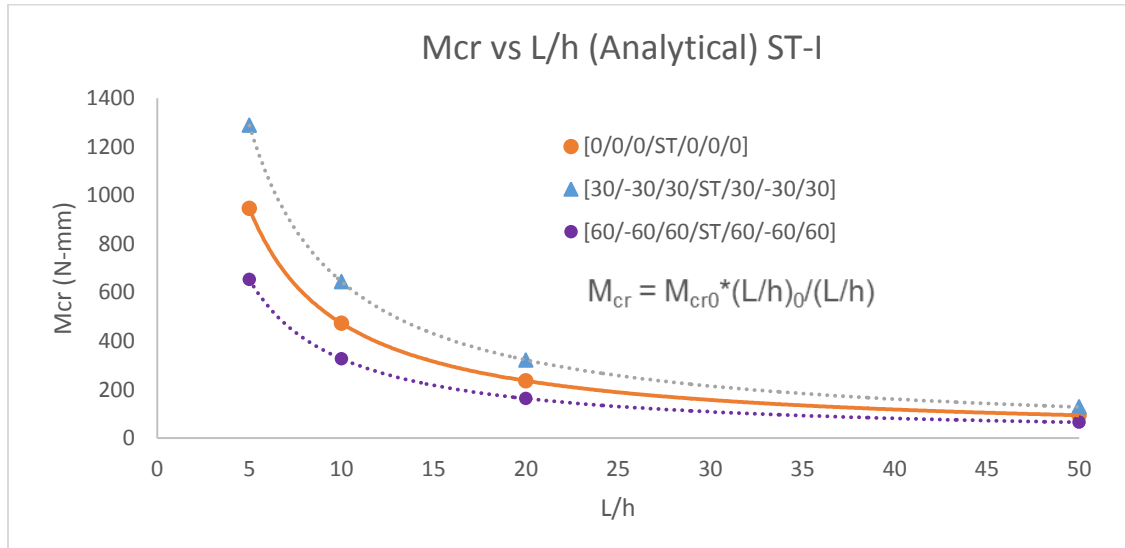


Figure 10: Effect of L/h ratio on the critical moment based on analytical formula for three different layups and layer thickness of 0.1 mm and ST-I arrangement.

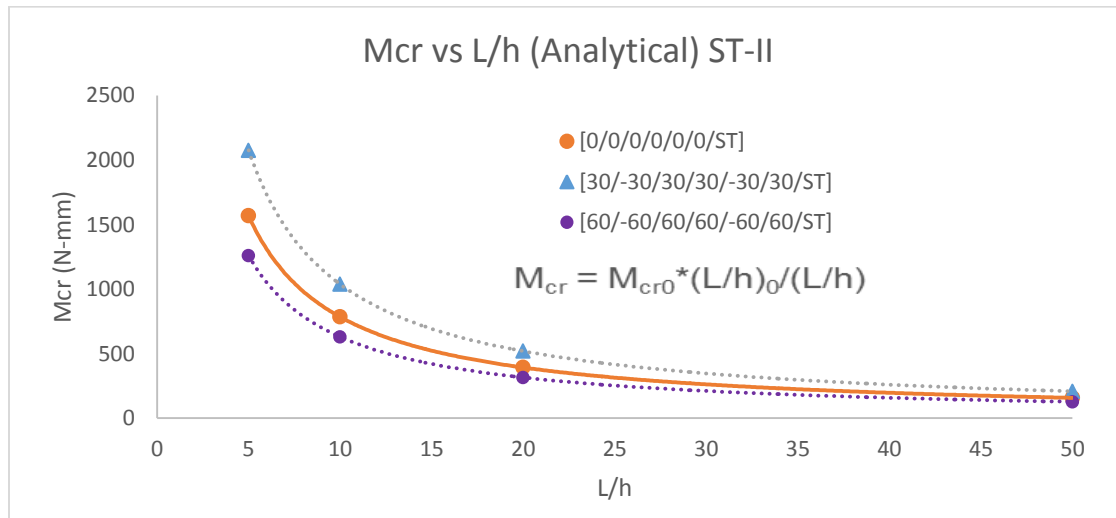


Figure 11: Effect of L/h ratio on the critical moment based on analytical formula for three different layups and layer thickness of 0.1 mm and ST-II arrangement.

By knowing the value of buckling moment in a selected laminate, Eq. 30 helps to calculate the buckling moment for different L/h ratios. Figure 10 show the effect of L/h ratio on the buckling moment for three different orientation sequences of ST-I type for [0/0/0/ST/0/0/0], [30/-30/30/ST/30/-30/30], and [60/-60/60/ST/60/-60/60] and ST-II type for [0/0/0/0/0/0/ST], [30/-30/30 /30/-30/30/ST], and [60/-60/60 /60/-60/60/ST]. Eq. 30 is limited to the analytical formula and is not applicable to the FEM results. There is a noticeable discrepancy between the analytical and numerical results in the cases of [0/0/0/ST/0/0/0] and [0/0/0/0/0/0/ST] laminates as the ratio of L/h decreases, as shown in Figure 13 and 14. This discrepancy is related to the fact that the

beam with zero fiber orientations buckles numerically in a distortional mode, in which the lateral angle of curvature at a certain section transverse the beam is not constant, rather than a lateral-torsional mode, in which the lateral angle of curvature remains constant for a certain section transverse to the beam, Fig. 12. Nevertheless, Figure 13 and 14 clearly show that the analytical and numerical buckling moments match almost exactly as the L/h ratio increases beyond 5 for both stacking sequences. It is obvious that in both analytical and FEM the buckling moments increase as the L/h ratio decrease because of the larger height of the beam to resist against lateral-torsional buckling.

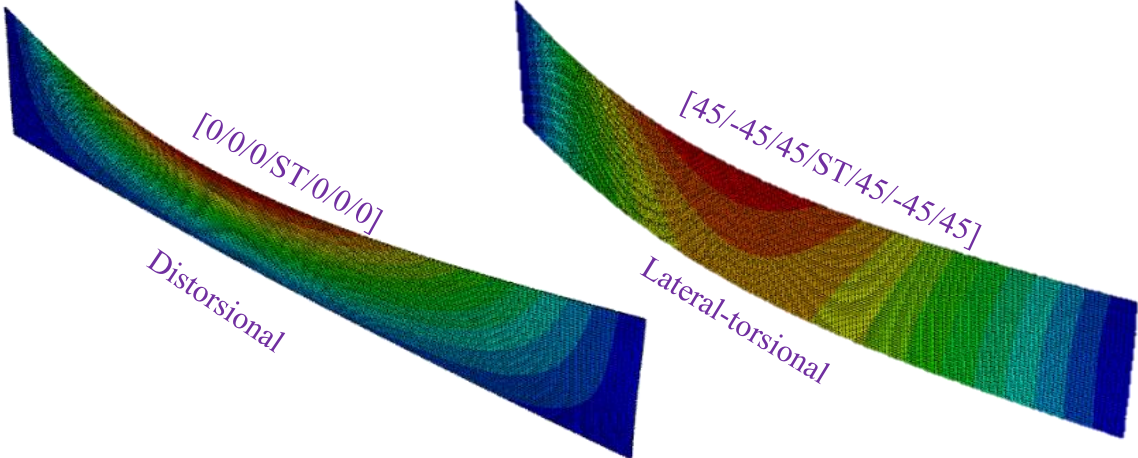


Figure 12: Buckling shapes showing distortional buckling mode and lateral-torsional buckling mode for ST-I arrangement

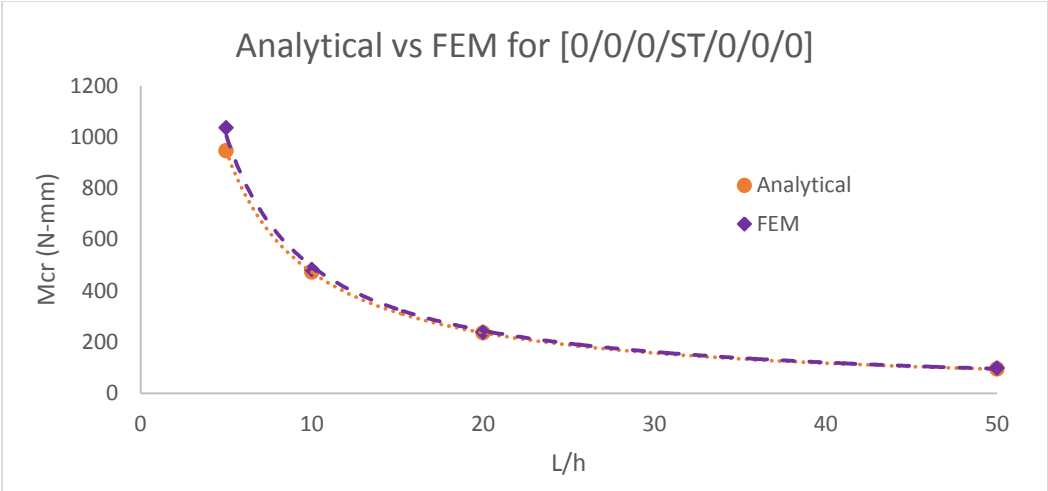


Figure 13 Comparison of buckling results obtained from analytical solution and FEM for the [0/0/0/ST/0/0/0] (ST-I) laminate and layer thickness of 0.1 mm by changing L/h ratio

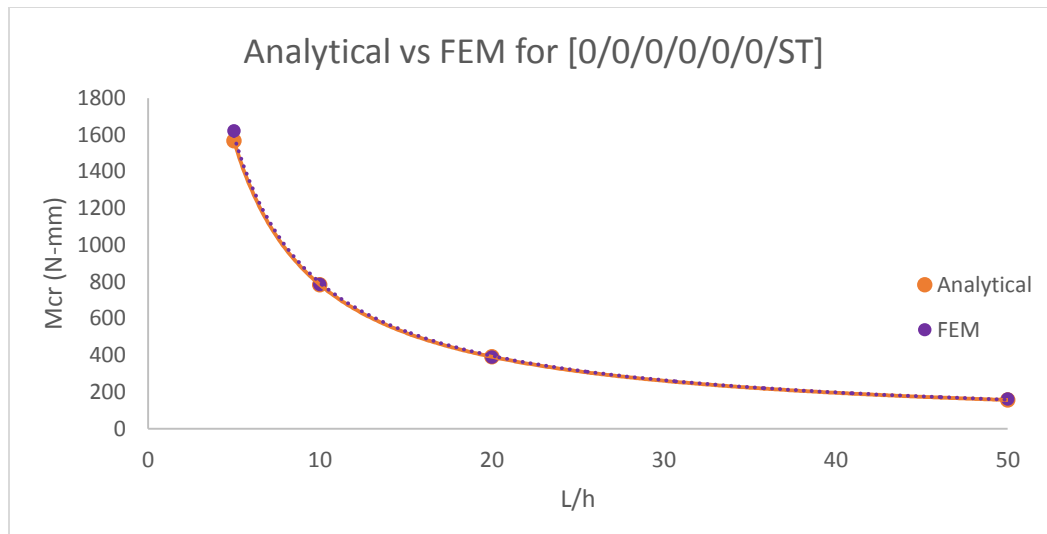


Figure 14: Comparison of buckling results obtained from analytical solution and FEM for the [0/0/0/0/0/0/ST] (ST-II) laminate and layer thickness of 0.1 mm by changing L/h ratio

5.2 Effect of stacking sequence (ST-I and ST-II)

The previous sections of this paper discussed the accuracy of the proposed analytical solution for hybrid beams against the finite element method for lateral-torsional buckling. Also, the effect of beam's size was examined against the buckling moment. In this section, and after verifying the accuracy of the solution, the two different stacking techniques are studied. Fig. 15 shows the ratios of the critical lateral torsional buckling moments for ST-II and ST-I for different fiber orientations. The figure shows ratios bigger than one, which lead to the conclusion that the ST-II, in which the steel sheet is at the side of the beam, has a higher resistance against lateral torsional buckling than the ST-I, in which the steel sheet is in the middle, for all examined fibers orientations.

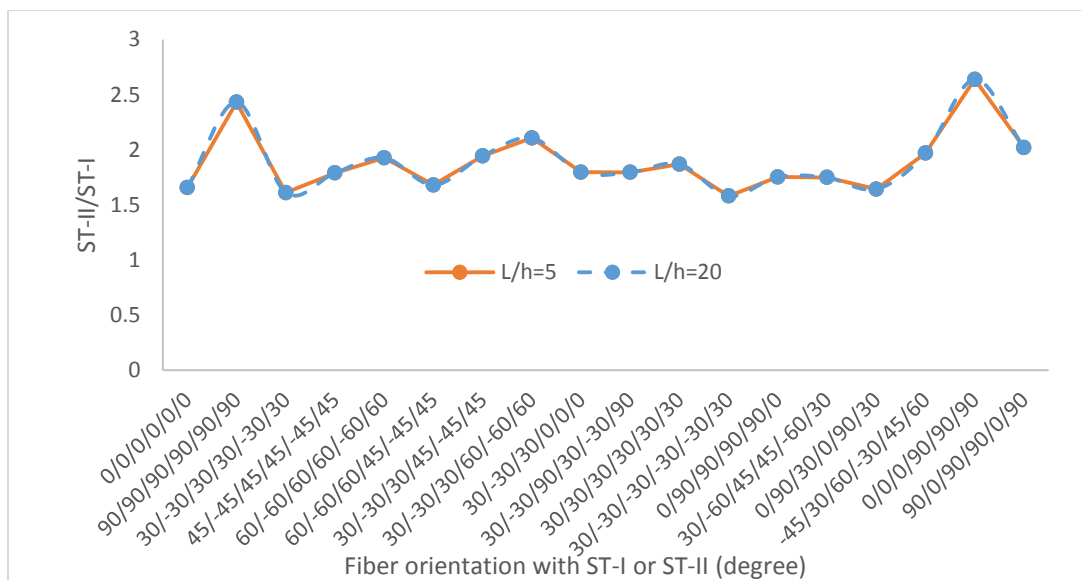


Figure 15: Normalized ST-II/ST-I vs the stacking sequence with L/h = 5 and L/h = 20

5.3 Effect of fiber angle orientation

As shown in Figure 6. The stacking sequences considerably affect the buckling moments if the dimensions of the beam are kept the same. The lowest value for the critical buckling moment is obtained when the fiber is perpendicular to the beam length while the highest critical value is obtained for the balanced angle-ply stacking sequence of 30 degrees which is the maximum critical moment among the possible stacking sequences selected for Figure 6. Furthermore, a comparison was held to study the effect of fiber angle on critical buckling load. The orientation $[\theta/-\theta/\theta/ST/\theta/-\theta/\theta]$ (degree) for ST-I and $[\theta/-\theta/\theta/\theta/-\theta/\theta/ST]$ (degree) for ST-II were examined with the change in layup angle of 0 to 90 with an increment of 5 degrees, Fig.16 and 17. The optimal maximum critical moment is obtained for the balanced angle-ply layup to be around 2100 N.mm for layup $[20/-20/20/20/-20/20/ST]$.

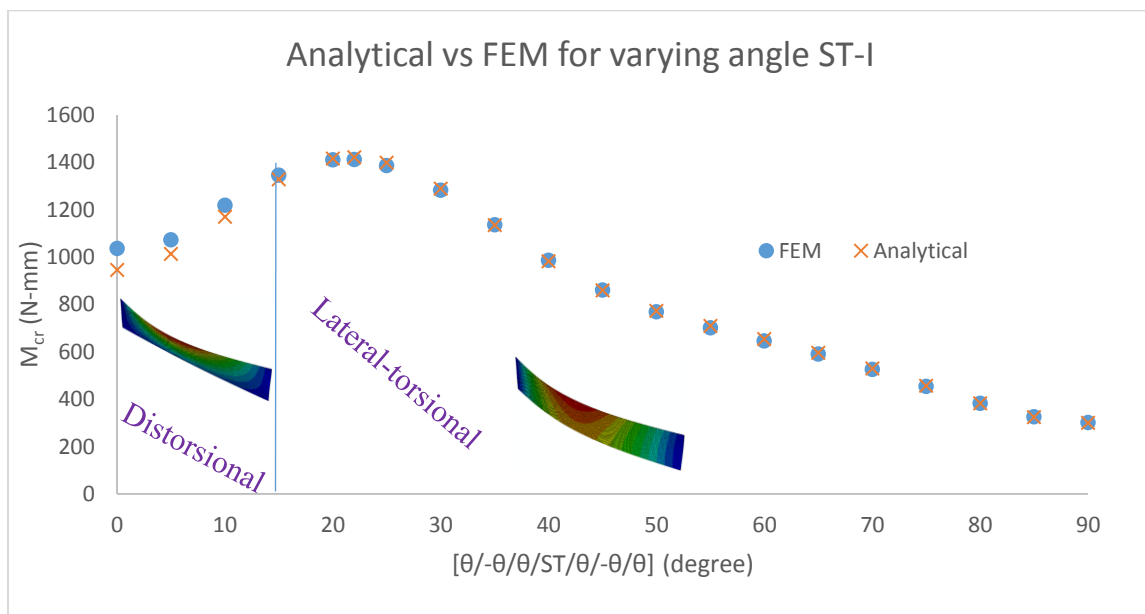


Figure 16: Variation in critical buckling moment with the change in layup angle of 0 to 90 at an increment of 5 degrees. (+) Analytical and (●) FEM; layer thickness of 0.1 mm and L/h of 5, ST-I

6. Conclusions

In this study, the lateral-torsional buckling of simply supported anisotropic hybrid (steel-FRP), thin-walled, rectangular cross-section beams under pure bending condition was investigated. Based on the assumptions made and the results obtained, an excellent accuracy is observed for a variety of stacking sequences. The applicability of this analytical formulation is proved by comparing the obtained results with FEM results. The study followed the classical laminated plate theory with all considered assumptions and determined an effective lateral-torsional-coupling stiffness matrix.

Based on the study, the stability of the laminated beams under pure bending is greatly affected by the length/height ratio of the beam. The critical buckling moment was inversely proportional to the length/height ratios with a power function. The lowest L/h ratio yields to the highest critical buckling moment. The importance of the stacking sequence, which does not affect the dimensions of the beam, is seen to greatly influence the stability of the beam. The ST-II stacking

type, in which the steel laminate is on the side of the beam, shows a higher resistance than the ST-I, in which the steel sheet is located at mid-thickness of the beam.

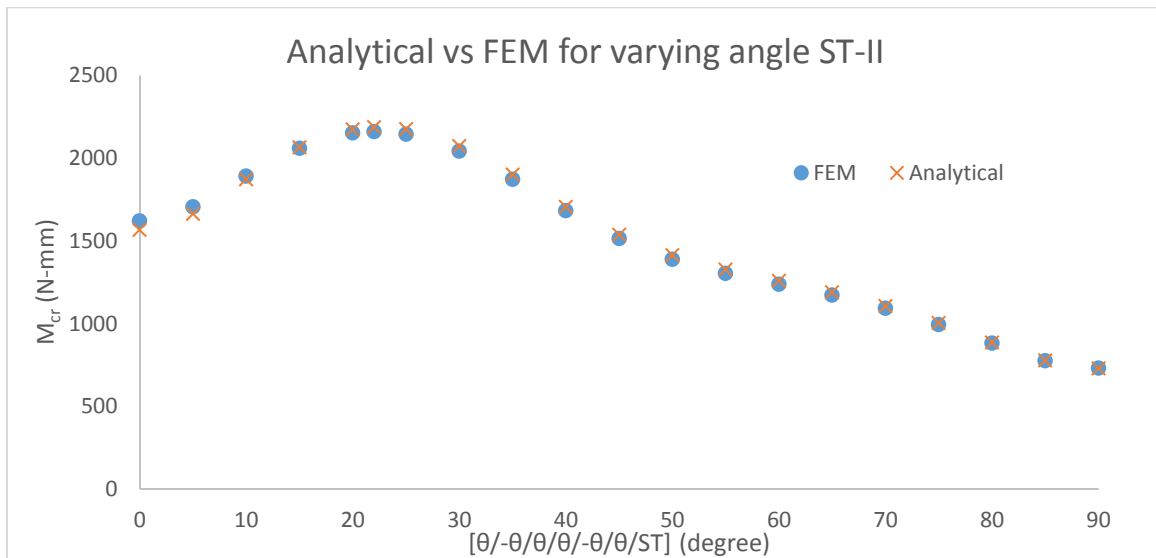


Figure 17: Variation in critical buckling moment with the change in layup angle of 0 to 90 at an increment of 5 degrees. (+) Analytical and (●) FEM; layer thickness of 0.1 mm and L/h of 5, ST-II

The fiber angle orientation was proven to be a critical variable against the lateral torsional buckling. The critical buckling moment of balanced angle-ply fiber lamination of about [20/-20/20/20/-20/20/ST] is found to reach the maximum value, among this class of layups, because of its maximum lateral and torsional effective stiffness. The minimum critical buckling moment obtained from [90/90/90/ST/90/90] was found to be due to orienting the fibers in the y-direction, thus reducing the lateral and torsional effective stiffness.

References

- BANK, L. C., & BEDNARCZYK, P. J. (1988). "A BEAM THEORY FOR THIN-WALLED COMPOSITE BEAMS". COMPOSITES SCIENCE AND TECHNOLOGY, VOL. 32, No.4, PP. 265-277
- BARBERO, E. J. (1999). "INTRODUCTION TO COMPOSITE MATERIALS DESIGN". CRC PRESS.
- BARBERO, E. J., LOPEZ-ANIDO, R., AND DAVALOS, F. (1993). "ON THE MECHANICS OF THIN-WALLED LAMINATED COMPOSITE BEAMS." JOURNAL OF COMPOSITE MATERIALS, VOL. 27, No.8, PP.806-829
- C. KARAAGAC, H. OZTURK, M. SABUNCU. (2007). "LATERAL DYNAMIC STABILITY ANALYSIS OF CANTILEVER LAMINATED COMPOSITE BEAM WITH AN ELASTIC SUPPORT". INTERNATIONAL JOURNAL OF STRUCTURAL STABILITY AND DYNAMICS. VOLUME 7, No. 3, PP. 377-402
- DAVALOS, J. F., AND QIAO, P. (1997), "ANALYTICAL AND EXPERIMENTAL STUDY OF LATERAL AND DISTORTIONAL BUCKLING OF FRP WIDE-FLANGE BEAMS", JOURNAL OF COMPOSITES FOR CONSTRUCTION, VOL. 1, PP. 150-159
- KARAAGAC, C., ÖZTÜRK, H., & SABUNCU, M. (2007). LATERAL DYNAMIC STABILITY ANALYSIS OF A CANTILEVER LAMINATED COMPOSITE BEAM WITH AN ELASTIC SUPPORT. INTERNATIONAL JOURNAL OF STRUCTURAL STABILITY AND DYNAMICS, VOL. 7, No.3, PP.377-402.
- KOLLÁR, L. P. (2001). "FLEXURAL-TORSIONAL BUCKLING OF OPEN SECTION COMPOSITE COLUMNS WITH SHEAR DEFORMATION." INTERNATIONAL JOURNAL OF SOLIDS AND STRUCTURES, No.38, PP. 7525-7541
- KOLLÁR, L. P., & SPRINGER, G. S. (2003). MECHANICS OF COMPOSITE STRUCTURES. CAMBRIDGE UNIVERSITY PRESS.
- KOTELKO, M. (2004). "LOAD-CAPACITY ESTIMATION AND COLLAPSE ANALYSIS OF THIN-WALLED BEAMS AND COLUMNS—RECENT ADVANCES". THIN-WALLED STRUCTURES, VOL. 42, No.2, PP.153-175
- LEE, J., KIM, S.-E., HONG, K. (2002). "LATERAL BUCKLING OF I-SECTION COMPOSITE BEAMS." ENGINEERING STRUCTURES, No. 24, PP. 955-964

- LIN, Z. M., POLYZOIS, D., AND SHAH, A. (1996). "STABILITY OF THIN-WALLED PULTRUDED STRUCTURAL MEMBERS BY THE FINITE ELEMENT METHOD." THIN-WALLED STRUCTURES, NO. 24, PP. 1-18
- MACHADO, S. P. (2010). "INTERACTION OF COMBINED LOADS ON THE LATERAL STABILITY OF THIN-WALLED COMPOSITE BEAMS." ENGINEERING STRUCTURES, NO. 32, PP. 3516-3527
- PANDEY, M.D., KABIR, M.Z., AND SHERBOURNE, A.N. (1995). "FLEXURAL-TORSIONAL STABILITY OF THIN-WALLED COMPOSITE I-SECTION BEAMS." COMPOSITES ENGINEERING, VOL. 5, NO.3, PP.321-342
- QIAO, P., ZOU, G., AND DAVALOS, J. (2003). "FLEXURAL-TORSIONAL BUCKLING OF FIBER-REINFORCED PLASTIC COMPOSITE CANTILEVER I-BEAMS." COMPOSITE STRUCTURES, NO. 60, PP. 205-217
- ROBERTS, T.M., AL-UBAIDI, H. (2001). "INFLUENCE OF SHEAR DEFORMATION ON RESTRAINED TORSIONAL WARPING OF PULTRUDED FRP BARS OF OPEN CROSS-SECTION." THIN-WALLED STRUCTURES, NO.39, PP. 395-414
- SAPKÁS, Á., & KOLLÁR, L. P. (2002). LATERAL-TORSIONAL BUCKLING OF COMPOSITE BEAMS. INTERNATIONAL JOURNAL OF SOLIDS AND STRUCTURES, VOL. 39, NO.11, PP. 2939-2963.
- SHERBOURNE, A. N., KABIR, M. Z. (1995). "SHEAR STRAIN EFFECTS IN LATERAL STABILITY OF THIN-WALLED FIBROUS COMPOSITE BEAMS." JOURNAL OF ENGINEERING MECHANICS, PP. 640-647.
- TAI, W. T. (2004). THE LATERAL-TORSIONAL BUCKLING ANALYSIS OF COMPOSITE LAMINATED BEAMS, MSc THESIS, FENG CHIA UNIVERSITY, TAIWAN ROC.
- TIMOSHENKO, S. P., & GERE, J. M. (1961). THEORY OF ELASTIC STABILITY. 1961.MCGRAWHILL-KOGAKUSHA LTD, TOKYO.
- VLISSOV, V. Z. (1961). THIN-WALLED BEAMS (2ND EDN) ISRAEL PROGRAM FOR SCIENTIFIC TRANSLATION.